Letters

Individual Phase Current Control With the Capability to Avoid Overvoltage in Grid-Connected Photovoltaic Power Plants Under Unbalanced Voltage Sags

Mitra Mirhosseini, Josep Pou, and Vassilios G. Agelidis

***Abstract*—Independent current control of each phase of a three-phase voltage source inverter under unbalanced voltage sags is proposed to effectively meet grid code requirements for grid-connected photovoltaic power plants (GCPPPs). Under current grid codes, GCPPPs should support grid voltages by injecting reactive currents during voltage sags. Such injection must not allow the grid voltages of the nonfaulty phases to exceed 110% of their nominal value. However, grid overvoltages can occur in the nonfaulty phases, especially if the currents injected into the grid by the GCPPP are balanced. Based on a new requirement of the European network of transmission system operators published in 2012, a transmission system operator is allowed to introduce a requirement for unbalanced current injection. In this letter, this grid code is addressed by controlling individual phases and injecting unbalanced currents into the grid during voltage sags. Experimental results from a 2.8-kV·A inverter are presented, confirming the effectiveness of the proposed control method.**

***Index Terms*—Photovoltaic system, power system faults, reactive current control.**

I. Introduction

THE control of grid-connected voltage source inverters (VSIs) under unbalanced voltage sags has been widely addressed in the technical literature. Some research has focused on active power control strategies, and two methods have been presented to provide the current references for the VSIs [1], [2]. As in the case of synchronous generators in conventional power plants, VSIs should remain connected during voltage sags and support the grid voltages with the injection of reactive currents [3], [4]. This is necessary to ride-through any type of fault.

The injection of balanced reactive currents to support unbalanced voltage sags may lead to overvoltages in the nonfaulty phases [5]. To prevent this, new grid codes (GCs) require the injection of unbalanced reactive currents during unbalanced voltage sags, and for this purpose different control methods have been proposed. In [6] and [7], a flexible voltage support method was introduced based on the type and severity of the voltage sags. For this purpose, the amount of reactive power injected via positive- and negative-sequences is controlled with an offline control parameter. An extended generalization of previous studies was carried out in [8], whereby the reactive power reference and the control parameter were updated in order to restore the dropped voltage amplitudes. Another study in [9] proposed a method to set the positive- and negative-sequence reactive power references based on an equivalent impedance grid model to avoid over- and undervoltages in the phases. In that paper, the new current references were updated based on the previous reactive power references. A decoupled double synchronous reference frame current controller was introduced in [10], with the capability of controlling the active and reactive power of the positive- and negative-sequences independently. However, the current references were regulated offline. Regarding the individual control of currents and voltages of the three phases, the new requirement of the European network of transmission system operators (TSOs) implies that TSOs are allowed to introduce a requirement for unbalanced current injection [11]. Few papers have studied or reported this concept to date. Some research was reported in [12] to support the phases with unbalanced reactive power. However, the method used in that paper was not universal for all types of voltage sags [13].

The objective of this letter is to propose a control method based on individual control of the phase currents under unbalanced voltage sags. The amount of reactive current in each phase is determined based on the amount of voltage drop in that phase, which implies no reactive current injection for the nonfaulty phases. Implementation of this method requires knowledge of the grid-voltage angle of each phase. For this purpose, the phase-locked loop (PLL) proposed in [14] is used. Moreover, the grid currents, including both active and reactive currents, are limited in order to protect the grid-connected photovoltaic power plants (GCPPPs) from ac overcurrents, addressing the fault-ride-through requirement. Since the grid currents are defined independently for each phase, two methods are proposed to prevent the controllers from trying to inject a zero-sequence into the grid. In this study, the proposed control technique was tested experimentally in a scaled-down GCPPP connected to a low-voltage (LV) programmable ac power supply.

The remainder of this letter is organized as follows: Section II introduces the synchronization method used to extract the phase angles of the grid voltages individually. Generation of the

Manuscript received December 21, 2014; revised February 4, 2015; accepted February 23, 2015. Date of publication March 5, 2015; date of current version May 22, 2015.

M. Mirhosseini and V. G. Agelidis are with the Australian Energy Research Institute and the School of Electrical Engineering and Telecommunications, The University of New South Wales, Sydney, N.S.W. 2052, Australia (e-mail: m.mirhosseini@student.unsw.edu.au; vassilios.agelidis@unsw.edu.au).

J. Pou is with the Australian Energy Research Institute and the School of Electrical Engineering and Telecommunications, The University of New South Wales, Sydney, N.S.W. 2052, Australia, on leave from the Technical University of Catalonia, 08222 Terrassa, Catalonia, Spain (e-mail: josep.pou@upc.edu).

Color versions of one or more of the figures in this paper are available online at http://ieeexplore.ieee.org.

Digital Object Identifier 10.1109/TPEL.2015.2410285

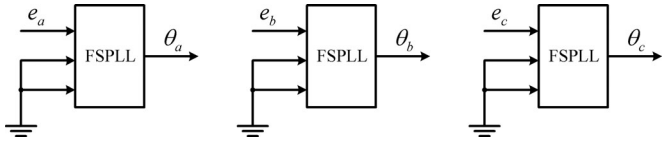

Fig. 1. Individual phase angle extraction based on the FSPLL.

current references is described in Section III, whereby a two-stage current limiter and two methods for eliminating the zero-sequence from the current references are proposed. The grid currents are regulated using proportional-resonant (PR) controllers and presented in Section IV. Experimental results from a scaled-down laboratory prototype with the proposed control method are presented in Section V. Finally, Section VI summarizes the main conclusions of this letter.

II. Single-Phase PLL Phase Extraction for Three-Phase Systems

As the aim of the proposed method is to control the phase currents independently, it is necessary to extract the phase angle of each of the grid voltages. Therefore, the frequency-adaptive PLL is implemented based on the research in [14]. This PLL is based on the filtered-sequence PLL (FSPLL) introduced in [15]. The first stage of the FSPLL separates the positive sequence of the grid voltages from the negative sequence and some harmonics by means of an asynchronous d-q transformation and moving average filters. The FSPLL includes a standard synchronous reference frame PLL to obtain the angle of the extracted positive sequence. In [14], three FSPLLs were used to detect the angles of the three-phase system i.e., θ_a, θ_b, and θ_c, for phase a, b, and c, respectively, as shown in Fig. 1. A single-phase voltage is introduced to each FSPLL, while the other inputs are set to zero as follows: $e_{a0} = (e_a, 0, 0)$, $e_{b0} = (e_b, 0, 0)$, and $e_{c0} = (e_c, 0, 0)$, in which e_a, e_b, and e_c are the grid voltages.

III. Generation of Phase Current References

In this section, the method for obtaining the current references to feed the current control loops is presented. The amplitude of the active current ($\hat{i}_A$) is defined to regulate the dc-link voltage, while the individual reactive current amplitudes ($\hat{i}_{R-x}$) are found from the droop control defined as

$$\hat{i}_{R-x} = droop\,|de_x|\,\hat{I}_n, \quad \text{with } x \in \{a,b,c\}$$
$$\text{for } \frac{|de_x|}{E_{n-ph}} \geq 10\% \quad \text{and} \quad droop \geq 2 \tag{1}$$

where $|de_x|$ is the amount of phase voltage drop from its nominal rms value (E_{n-ph}), $\hat{I}_n$ is the amplitude of the nominal phase current of the inverter, and $droop$ is a constant value based on the German GCs [4]. A value ≥ 2 for $droop$ implies that, for voltage support, the injection of reactive current at the LV side of the transformer must be at least 2% of the nominal current per each percent of the voltage drop [4]. The dc-link voltage loop is controlled by a proportional-integral (PI) controller equipped with an antiwindup technology that helps attain the prefault values very quickly after fault removal. This can be seen in the control diagram of Fig. 2. In this figure, $v_{\rm dc}$ is the dc-link voltage, $V^*_{\rm dc}$ is its reference value, and i^*_d is the active current reference in the dq-reference frame.

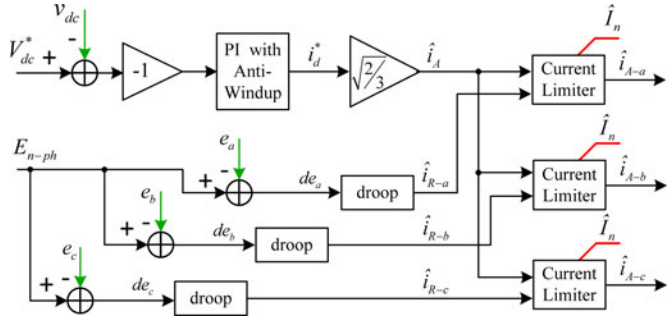

Fig. 2. Control diagram for obtaining the active and reactive current references.

A. Limiting the Phase Currents

Under a voltage sag condition, the controller increases the active currents to maintain the power injected into the grid. At the same time, reactive current needs to be injected into the faulty phases to support the grid voltages. Consequently, the total phase currents may increase above the maximum acceptable values, which would eventually trigger the overcurrent protection. To avoid this situation, priority is given to the reactive current injection to support the grid voltages. Therefore, the amplitudes of the active currents are limited based on the reactive current required for each phase (see Fig. 2). The priority under a voltage sag is to support the grid voltages with the injection of reactive currents. However, the current of each phase cannot go beyond the maximum acceptable value defined for the inverter. Therefore, in the case of overcurrent in one phase, the active current of that phase should be limited. The current limiter in Fig. 2 is defined as follows:

$$\hat{i}_{A-x} = \begin{cases} \hat{i}_A, & \text{if } \sqrt{\hat{i}^2_{R-x} + \hat{i}^2_A} \leq \hat{I}_n \text{ and} \\ \sqrt{\hat{I}^2_n - \hat{i}^2_{R-x}}, & \text{if } \sqrt{\hat{i}^2_{R-x} + \hat{i}^2_A} > \hat{I}_n \end{cases} \tag{2}$$

where x stands for phases a, b, and c. The actual current reference for each phase is obtained by multiplying the amplitudes of the active and reactive currents by the cosine and sine, respectively, of the phase angle obtained from the PLLs [14]. The final current reference for each phase is achieved by adding the active and reactive current components. Fig. 3 illustrates the procedure for obtaining the current reference i^*_a for phase a. The current references for the other phases are obtained using the same procedure.

B. Zero-Sequence Elimination from the Current References

Since the currents of the three phases are regulated independently, the sum of the three currents may not be zero. This would mean circulation of a zero-sequence current component through the ground. This cannot happen if the ground circuit is open. Furthermore, if the ground circuit offers a low impedance, circulation of this current may not be a desired situation.

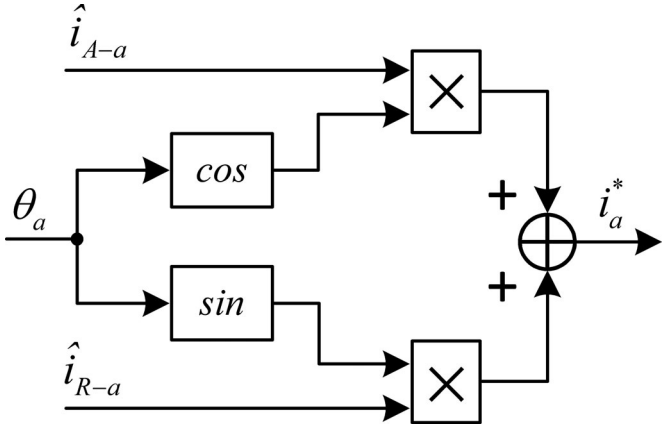

Fig. 3. Current reference generation for phase a.

Therefore, this zero-sequence should be removed from the current references.

This can be achieved by applying the Clarke transformation ($abc/\alpha\beta$) to the current references. In this case, the third component in the Clarke transformation, i.e., the γ or zero-sequence component, is disregarded. As a result, the current vector will lie in the $\alpha\beta$ plane, coinciding with its projection before the zero-sequence was removed. Therefore, the $\alpha\beta$ components of the reference currents will be preserved.

An equivalent way of removing the zero-sequence is changing the current references of each phase by subtracting one-third of the common current component from each of them as follows:

$$i_a^{*'} = i_a^* - k_a i_0 \tag{3}$$

$$i_b^{*'} = i_b^* - k_b i_0 \tag{4}$$

$$i_c^{*'} = i_c^* - k_c i_0 \tag{5}$$

where

$$i_0 = i_a^* + i_b^* + i_c^* \text{ and} \tag{6}$$

$$k_a = k_b = k_c = 1/3. \tag{7}$$

During balanced operation, the common component i_0 will be zero or very low. However, during unbalanced voltage sags, the common component may have a significant value. Consequently, after applying (3)–(7), the new references $i_a^{*'}$, $i_b^{*'}$, and $i_c^{*'}$ may differ with respect to the original values. Therefore, the reactive components of the nonfaulty phases may increase, causing a voltage rise above the limits. An alternative solution to avoid this problem is explained below.

The proposed solution is based on changing the current references depending on the activation of the reactive current injection for each phase, keeping the reference(s) of the phase(s) with no reactive current injection unchanged. For example, if phase a is nonfaulty under an unbalanced voltage sag, k_a will be set to zero, and the zero-sequence is eliminated by changing the current references of the other phases, i.e., $k_b + k_c = 1$. In this letter, the zero-sequence elimination is divided equally between the faulty phases, i.e., $k_b = k_c = 1/2$.

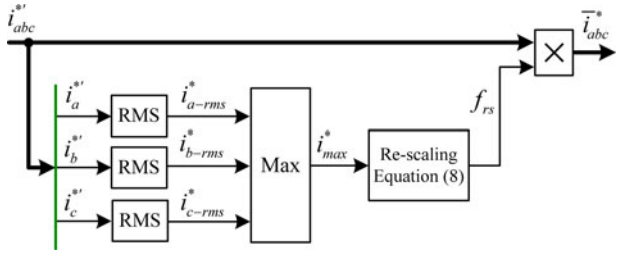

Fig. 4. Control diagram for rescaling the current references to avoid overcurrents.

C. Second Current Limiter

Once the zero-sequence component is removed from the current references, the amplitudes of the currents change, which may produce overcurrents. To limit the phase currents at or below the maximum value (I_n), a method to measure the rms value of the currents should be implemented. The following equation can be used for this:

$$i_{x-\text{rms}}^* = \sqrt{\frac{1}{T_w}\int_{t-T_w}^{t} (i_x^{*'})^2 \, \mathrm{d}t} \tag{8}$$

in which $i_{x-\text{rms}}^*$ is the rms value of the phase current x, where x represents the three phases ($x \in \{a, b, c\}$), and T_w is the window width used for the rms calculation, typically $T/2$ or T, T being the grid-voltage period ($T = 1/\text{freq}$). The maximum current of the three phases (i_{max}^*) is compared with the nominal value I_n. If it exceeds I_n, all the currents are rescaled by a factor f_{rs} defined as

$$f_{\text{rs}} = \begin{cases} \frac{I_n}{i_{\text{max}}^*}, & \text{if } i_{\text{max}}^* > I_n \\ 1, & \text{if } i_{\text{max}}^* \le I_n. \end{cases} \tag{9}$$

The final current references are set as follows:

$$\bar{i}_{abc}^* = f_{rs} i_{abc}^{*'}. \tag{10}$$

The proposed method for rescaling the currents is illustrated in Fig. 4. The magnitudes indicated with the subscript "abc" represent the three phase magnitudes of the system, e.g., i_{abc} stands for i_a, i_b, and i_c.

The process of generating the phase current references includes two limiters. The first one, shown in Fig. 2, is to limit the active currents to give enough room to the required reactive current injection. The second one is based on rescaling all the current references after the zero-sequence elimination. This process is proposed here for the first time and has never been addressed in any other study.

IV. Current Control Loop

The current control is composed of two parallel loops that regulate the currents in a stationary frame. Since the control variables are sinusoidal, PR controllers were chosen, as conventional PI controllers fail to remove steady-state errors when controlling sinusoidal waveforms. The control diagram of the currents is shown in Fig. 5. The inputs to this control diagram are the current references obtained from (10).

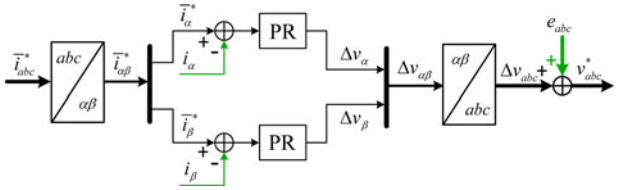

Fig. 5. Current control loop with PR controllers.

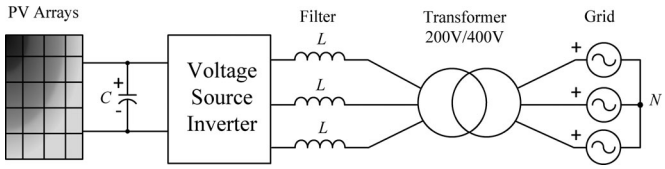

Fig. 6. Diagram of a GCPPP.

TABLE I
EXPERIMENTAL SETUP CHARACTERISTICS

Injected power from PV array	2.8 kW	Transformer	5 kVA, 400/200 V Dyn11, 50 Hz
Maximum operating voltage, $V_{m\,pp}$	393 V	Transformer leakage inductance (LV side), L_{trans}	0.9 mH/phase
DC-link capacitor, C	1100 μF	Total grid inductance, $L_g = L'_g + L_{\text{trans}}$	1.9 mH/phase
Switching frequency, f_s	10 kHz	Filter inductance, L	4 mH/phase

V. EXPERIMENTAL STUDIES

A. Experimental Setup

The proposed control method was tested in a scaled-down GCPPP. The scheme of the GCPPP is presented in Fig. 6 and the main specifications are summarized in Table. I.

To illustrate the impact of injecting reactive power on the grid-voltage magnitudes, a weak grid is required. In this study, a weak grid was emulated by adding inductors to the LV side of the transformer (L'_g). The inductance L_g shown in Fig. 7 includes the added inductance and the transformer inductance reduced to the LV side (L_{trans}), i.e., $L_g = L'_g + L_{\text{trans}}$. The grid voltages are measured between the inductors L and L_g (indicated by $\overrightarrow{E_g}$ in Fig. 7) and used for PLL synchronization. In the steady state, $\overrightarrow{E_g}$ can be obtained as follows:

$$\overrightarrow{E_g} = \frac{1}{1+k}(k\overrightarrow{V} + \overrightarrow{E}) \tag{11}$$

where $k = L_g/L$.

The lower the value of k, the lower the amplitude of the switching frequency components in $\overrightarrow{E_g}$. However, k should not be too small, otherwise the injection of reactive currents will have no significant effect on the voltage $\overrightarrow{E_g}$. Fig. 8 shows how the inductances can help to increase the voltage $\overrightarrow{E_g}$ when injecting reactive current.

As the power flows from the inverter to the grid, $\overrightarrow{V}$ is always greater than $\overrightarrow{E}$. The magnitude of $\overrightarrow{E_g}$ depends on the characteristics of the current injected into the grid, as depicted in Fig. 8. Since $L_g < L$, the magnitude of the voltage drop in

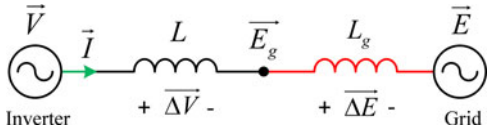

Fig. 7. Generation of a weak grid in the laboratory.

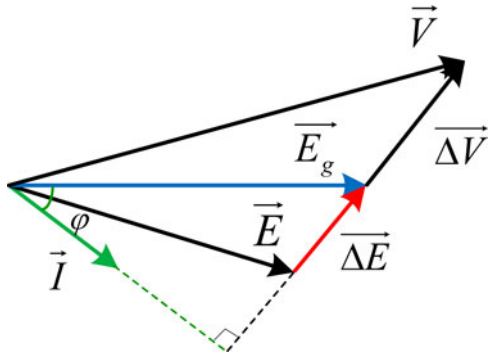

Fig. 8. Phasor diagram when the injected current is resistive-capacitive.

L_g is less than L, i.e., $|\Delta\overrightarrow{E}| < |\Delta\overrightarrow{V}|$. If the current injected is purely resistive ($\varphi = 0°$), the magnitude of the voltages can be sorted as $|\overrightarrow{E_g}| < |\overrightarrow{E}| < |\overrightarrow{V}|$. If the current injected is purely capacitive ($\varphi = 90°$) or resistive-capacitive ($0° < \varphi < 90°$ except for small angles φ), the voltage magnitudes can be sorted as $|\overrightarrow{E}| < |\overrightarrow{E_g}| < |\overrightarrow{V}|$. As a result, the magnitude of the voltage $\overrightarrow{E_g}$ can be increased above $|\overrightarrow{E}|$ when there is reactive current injection. This is the principle used to regulate the grid voltages through the injection of reactive current.

One can observe in Fig. 8 that if L_g were small (representing a strong grid), the voltages $\overrightarrow{E_g}$ and $\overrightarrow{E}$ would be almost the same, and therefore, $\overrightarrow{E_g}$ would have very limited control. On the other hand, if L_g is large (representing a weak grid), the voltage $\overrightarrow{E_g}$ can be significantly different than $\overrightarrow{E}$. The maximum difference between the magnitudes $|\overrightarrow{E_g}|$ and $|\overrightarrow{E}|$ is achieved when the current $\overrightarrow{I}$ is purely reactive, since the voltage drop $\Delta\overrightarrow{E}$ is aligned with $\overrightarrow{E_g}$ and $\overrightarrow{E}$. In this case, the voltage magnitude $|\overrightarrow{E_g}|$ is increased with respect to $|\overrightarrow{E}|$ by $|\Delta\overrightarrow{E}|$ ($|\Delta\overrightarrow{E}| = |\overrightarrow{I}|\omega L_g$). From this point of view, the larger the L_g value the better. On the other hand, if L_g were equal or larger than L, significant voltage ripples would appear on the top of $\overrightarrow{E_g}$. This is one of the reasons why L_g should be smaller than L.

In order to calculate the inductances L and L'_g in the experimental setup, the amplitude of the current ripple ($\hat{I}_{\text{ripple}}$) is limited to be less than 10% of the amplitude of the fundamental component of the grid current under rated operating conditions ($\hat{I}_{\text{fund}}$), i.e.,

$$\hat{I}_{\text{ripple}} \leq 0.1\hat{I}_{\text{fund}}. \tag{12}$$

Considering the worst-case scenario for the current ripple, which is produced when the duty cycle of the phase-leg is 50%,

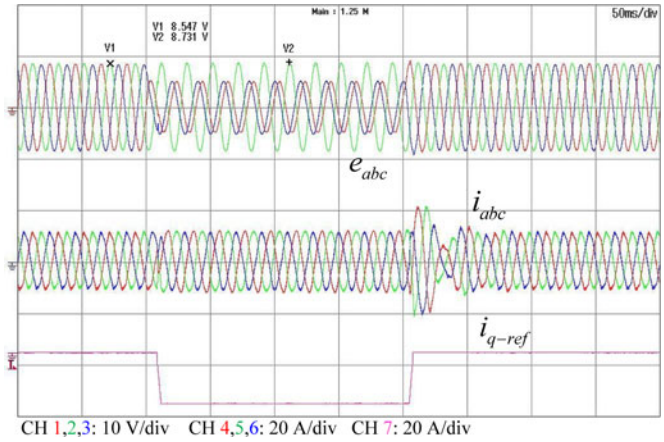

Fig. 9. Performance of the balanced control method for the GCPPP under a 100% LG voltage sag at the grid side of the transformer. From top to bottom: Grid voltages at the LV side of the transformer, output currents at the LV side, and reactive current reference.

the amplitude of the ripple is calculated by

$$\hat{I}_{\text{ripple}} = \frac{v_{\text{dc}}}{4(L+L_g)f_s} \tag{13}$$

where f_s is the switching frequency of the inverter. Substituting (13) into (12)

$$L + L_g \geq \frac{v_{\text{dc}}}{0.4\sqrt{2}I_{\text{rms}}f_s} \tag{14}$$

I_{rms} being the rms value of the output current under rated operating conditions. Substituting the values in Table I into (14)

$$L + L_g \geq 4.8 \text{ mH}. \tag{15}$$

From (15) and considering that the transformer inductance is $L_{\text{trans}} = 0.9$ mH and L has to be larger than L_g, i.e., $L > L_g = L'_g + L_{\text{trans}}$, L and L'_g are selected to be 4 and 1 mH, respectively.

B. Experimental Results

Experimental results were obtained by connecting the scaled-down GCPPP to the laboratory "weak" grid. First, balanced currents were injected. In this case, the lowest line-to-line voltage was considered for the droop control. This implies the injection of balanced reactive currents into all three phases. The detailed control method under balanced currents can be found in [16]. Fig. 9 shows the results obtained under a line-to-ground (LG) voltage sag with 100% voltage drop in phase a imposed at the grid side of the transformer. The voltage magnitudes are scaled down by a factor of 20 to be able to show them on the oscilloscope. As demonstrated, the injection of balanced reactive currents under unbalanced voltage sags leads to voltage rise in the nonfaulty phase. In this case, the amplitudes of the grid voltages rise from $8.547 \times 20 = 170.94$ V to $8.731 \times 20 = 174.63$ V, which equates to an increase of 1.84% of the grid voltages during the voltage sag. Although this value does not reach the limit defined by the GCs, this test shows the effect of raising the voltage of the nonfaulty phases above the nominal value.

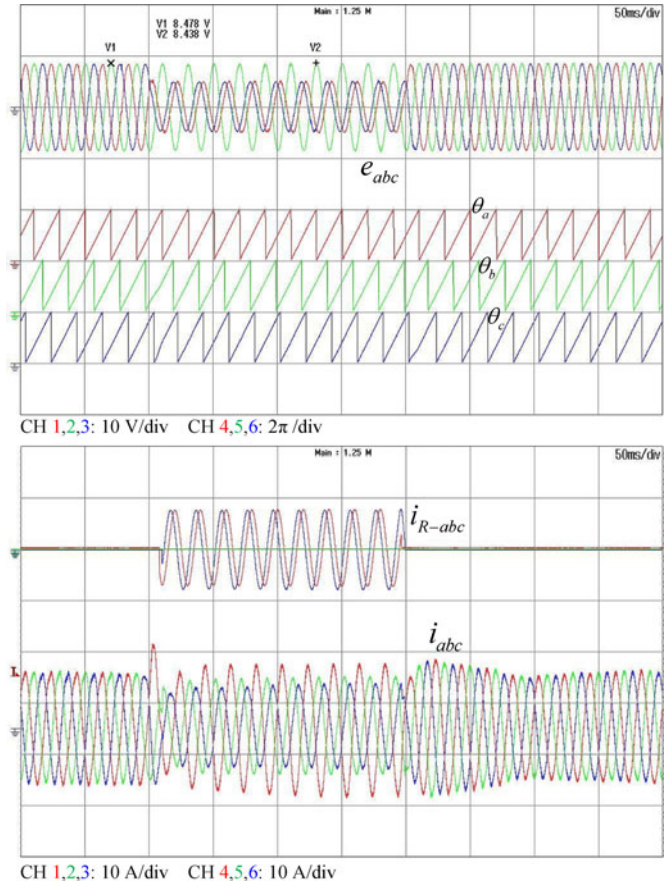

Fig. 10. Performance of the proposed control method under a 100% LG voltage sag at the grid side of the transformer. From top to bottom: Grid voltages at the LV side of the transformer, detected angles of phases a, b, and c, generated reactive current references, and output currents at the LV side.

The performance of the proposed method was demonstrated in the following test. Consider the same voltage sag as the one in the previous test. Since the LG voltage sag is of Type B, the respective voltage sag at the LV side of the transformer, after passing through a $Dyn11$ transformer, is a Type C voltage sag. As a result, the reactive current should be injected only into the two faulty phases at the inverter side. The results of this are shown in Fig. 10. In this case, since there is no injection of reactive current into the nonfaulty phase (green phase), there is no voltage rising in that phase, while the voltages of the other two phases rise owing to the injection of the appropriate reactive currents. Moreover, the current limiter proposed in Section III-C prevents the system from overcurrents.

VI. Conclusion

In this letter, a new control method based on individual control of the three phases of a GCPPP has been proposed. The independent control of the reactive currents injected into the grid protects the nonfaulty phases from overvoltage. The reactive currents are determined separately based on the amount of voltage drop in each phase. The active current references of each phase need to be limited based on the required amount of reactive currents. Furthermore, in a three-phase system, it is necessary to

eliminate the zero-sequence from the current references generated. In this letter, two solutions for removing the zero-sequence component have been proposed. Finally, a method for rescaling the instantaneous current references to avoid producing overvoltages in the nonfaulty phases, while preventing the GCPPP from overcurrents has also been proposed. This proposed control method has been tested experimentally on a scaled-down laboratory prototype operating with a "weak" grid.

REFERENCES

[1] P. Rodriguez, A. Timbus, R. Teodorescu, M. Liserre, and F. Blaabjerg, "Flexible active power control of distributed power generation systems during grid faults," *IEEE Trans. Ind. Electron.*, vol. 54, no. 5, pp. 2583–2592, Oct. 2007.

[2] F. Wang, J. Duarte, and M. Hendrix, "Design and analysis of active power control strategies for distributed generation inverters under unbalanced grid faults," *IET Gener., Trans. Distrib.*, vol. 4, no. 8, pp. 905–916, Aug. 2010.

[3] BDEW. (2008, Jun.). Technical guideline-generating plants connected to the medium-voltage network-guideline for generating plants connection to and parallel operation with the medium-voltage network [Online]. Available: https://www.bdew.de

[4] E. Troester, "New german grid codes for connecting PV systems to the medium voltage power grid," in *Proc. 2nd Int. Workshop Concentrating Photovoltaic Power Plants, Opt. Des., Prod. Grid Connection*, Mar. 2009, pp. 1–4.

[5] M. Mirhosseini, J. Pou, and V. G. Agelidis, "Single-stage inverter-based grid-connected photovoltaic power plant with ride-through capability over different types of grid faults," in *Proc. IEEE 39th Ann. Conf. Ind. Electron. Soc.*, Nov. 2013, pp. 8008–8013.

[6] A. Camacho, M. Castilla, J. Miret, J. Vasquez, and E. Alarcon-Gallo, "Flexible voltage support control for three-phase distributed generation inverters under grid fault," *IEEE Trans. Ind. Electron.*, vol. 60, no. 4, pp. 1429–1441, Apr. 2013.

[7] M. Castilla, J. Miret, A. Camacho, J. Matas, E. Alarcon-Gallo, and L. de Vicuna, "Coordinated reactive power control for static synchronous compensators under unbalanced voltage sags," in *Proc. IEEE Int. Symp. Ind. Electron.*, May, 2012, pp. 987–992.

[8] J. Miret, A. Camacho, M. Castilla, L. de Vicuna, and J. Matas, "Control scheme with voltage support capability for distributed generation inverters under voltage sags," *IEEE Trans. Power Electron.*, vol. 28, no. 11, pp. 5252–5262, Nov. 2013.

[9] A. Camacho, M. Castilla, J. Miret, R. Guzman, and A. Borrell, "Reactive power control for distributed generation power plants to comply with voltage limits during grid faults," *IEEE Trans. Power Electron.*, vol. 29, no. 11, pp. 6224–6234, Nov. 2014.

[10] M. Reyes, P. Rodriguez, S. Vazquez, A. Luna, R. Teodorescu, and J. Carrasco, "Enhanced decoupled double synchronous reference frame current controller for unbalanced grid-voltage conditions," *IEEE Trans. Power Electron.*, vol. 27, no. 9, pp. 3934–3943, Sep. 2012.

[11] European Network of Transmission System Operator (ENTSO). (2012, Jan.). Entso-e draft network code for requirements for grid connection applicable to all generators [Online]. Available: https://www.entsoe.eu/major-projects/network-code-development/requirements-for-generators/Pages/default.aspx

[12] A. Uphues, K. Notzold, R. Wegener, S. Soter, and R. Griessel, "Support of grid voltages with asymmetrical reactive currents in case of grid errors," in *Proc. IEEE Int. Conf. Ind. Technol.*, Feb. 2013, pp. 1781–1786.

[13] M. Bollen, *Understanding Power Quality Problems: Voltage Sags and Interruptions*. New York, NY, USA: Wiley-IEEE, 2000.

[14] M. Mirhosseini, J. Pou, V. G. Agelidis, E. Robles, and S. Ceballos, "A three-phase frequency-adaptive phase-locked loop for independent single-phase operation," *IEEE Trans. Power Electron.*, vol. 29, no. 12, pp. 6255–6259, Dec. 2014.

[15] E. Robles, S. Ceballos, J. Pou, J. Martin, J. Zaragoza, and P. Ibanez, "Variable-frequency grid-sequence detector based on a quasi-ideal low-pass filter stage and a phase-locked loop," *IEEE Trans. Power Electron.*, vol. 25, no. 10, pp. 2552–2563, Oct. 2010.

[16] M. Mirhosseini, J. Pou, and V. G. Agelidis, "Single- and two-stage inverter-based grid-connected photovoltaic power plants with ride-through capability under grid faults," to appear in *IEEE Trans. Sustain. Energy.*